Discontinuous Molecular Dynamics for Semi-Flexible and Rigid Bodies

Lisandro Hernández de la Peña, Ramses van Zon, Jeremy Schofield
Chemical Physics Theory Group, Department of Chemistry, University of Toronto, Ontario, Canada M5S 3H6

Sheldon B. Opps
Department of Physics, University of Prince Edward Island, 550 University Avenue, Charlottetown, Prince Edwards Island, Canada C1A 4P3

(Dated: July 20, 2006)

A general framework for performing event-driven simulations of systems with semi-flexible or rigid bodies interacting under impulsive torques and forces is outlined. Two different approaches are presented. In the first, the dynamics and interaction rules are derived from Lagrangian mechanics in the presence of constraints. This approach is most suitable when the body is composed of relatively few point masses or is semi-flexible. In the second method, the equations of rigid bodies are used to derive explicit analytical expressions for the free evolution of arbitrary rigid molecules and to construct a simple scheme for computing interaction rules. Efficient algorithms for the search for the times of interaction events are designed in this context, and the handling of missed interaction events is discussed.

I. INTRODUCTION

There has been an increasing interest over the last decade in performing large-scale simulations of colloidal systems, proteins, micelles and other biological assemblies. Simulating such systems, and the phenomena that take place in them, typically requires a description of dynamical events that occur over a wide range of time scales. Nearly all simulations of such systems to date are based on following the microscopic time evolution of the system by integration of the classical equations of motion. Usually, due to the complexity of inter-molecular interactions, this integration is carried out in a step-by-step numerical fashion producing a time ordered set of phase-space points (a *trajectory*). This information can then be used to calculate thermodynamic properties, structural functions or transport coefficients. An alternative approach, which has been employed in many contexts, is to use step potentials to approximate intermolecular interactions while affording the analytical solution of the dynamics [1, 2, 3, 4, 5]. The simplification in the interaction potential can lead to an increase in simulation efficiency since the demanding task of calculating forces is reduced to computing momentum exchanges between bodies at the instant of interaction. This approach is called event-driven or *discontinuous molecular dynamics* (DMD).

In the DMD approach, various components of the system interact via discontinuous forces, leading to impulsive forces that act at specific moments of time. As a result, the motion of particles is free of inter-molecular forces between impulsive *events* that alter the trajectory of bodies via discontinuous jumps in the momenta of the system at discrete interaction times. To determine the dynamics, the basic interaction rules of how the (linear and angular) momenta of the body are modified by collisions must be specified.

For molecular systems with internal degrees of freedom it is straightforward to design fully-flexible models with discontinuous potentials, but DMD simulations of such systems are often inefficient due to the relatively high frequency of internal motions[6]. This inefficiency is reflected by the fact that most collision events executed in a DMD simulation correspond to intra rather than inter-molecular interactions. On the other hand, much of the physics relevant in large-scale simulations is insensitive to details of intra-molecular motion at long times. For this reason, methods of incorporating constraints into the dynamics of systems with continuous potentials have been developed that eliminate high frequency internal motion, and thus extend the time scales accessible to simulation. Surprisingly, relatively little work has appeared in the literature on incorporating such constraints into DMD simulations. The goal of this paper is to extend the applicability of DMD methods to include constrained systems and to outline efficient methods that are generally applicable in the simulations of semi-flexible and rigid bodies interacting via discontinuous potentials.

In contrast to systems containing only simple spherical particles [4, 5, 6, 7, 8], the application of DMD methods to rigid-body systems is complicated by two main challenges. The first challenge is to analytically solve the dynamics of the system so that the position, velocity, or angular velocity of any part of the system can be obtained exactly. This is in principle possible for a rigid body moving in the absence of forces and torques, even if it does not possess an axis of symmetry which facilitates its motion. However, an explicit solution suitable for numerical implementation seems to be missing in the literature (although partial answers are abundant [9, 10, 11, 12, 13, 14]). For this reason, we will present the explicit solution here. Armed with a solution of the dynamics of all bodies in the system, one can calculate the collision times in an efficient manner, and in some instances, analytically.

The second challenge is to determine how the impulsive

forces lead to discontinuous jumps in the momenta of the interacting bodies. For complicated rigid or semi-flexible bodies, the rules for computing the momentum jumps are not immediately obvious. It is clear however that these jumps in momenta must be consistent with basic conservation laws connected to symmetries of the underlying Lagrangian characterizing the dynamics. Often the basic Lagrangian is invariant to time and space translations, and rotations, and, hence, the rules governing collisions must explicitly obey energy, momentum, and angular momentum constraints. Such conservation laws can be utilized as a guide to derive the proper collision rules.

A first attempt to introduce constraints into an event-driven system was carried out by Ciccotti and Kalibaeva[15], who studied a system of rigid, diatomic molecules (mimicking liquid nitrogen). Furthermore, non-spherical bodies of a special kind were treated by Donev *et al.*[16, 17] by assuming that all rotational motion in between interaction events was that of a spherically symmetric body. More recently, a spherically symmetric hard-sphere model with four tetrahedral short ranged (sticky) interactions (mimicking water) has been studied by De Michele *et al.*[18] with an event-driven molecular dynamics simulation method similar to the most basic scheme presented in this paper. This work primarily focuses on the phase diagram of this "sticky" water model as a prototype of network forming molecular systems. Our purpose, in contrast, is to discuss a general framework that allows one to carry out event-driven DMD simulations in the presence of constraints and, in particular, for fully general rigid bodies. The methodology is applicable to modeling the correct dynamics of water molecules in aqueous solutions[19] as well as other many body systems.

The paper is organized as follows. Section II discusses the equations of motions in the presence of constraints and Sec. III discusses the calculation and scheduling of collision times. The collision rules are derived in Sec. IV. In Sec. V it is shown how to sample the canonical and microcanonical ensembles and how to handle subtle issues concerning missing events that are particular to event-driven simulations. Finally, conclusions are presented in Sec. VI.

II. EQUATIONS OF MOTION WITH CONSTRAINTS

A. Constrained dynamics

The motion of rigid bodies can be considered to be a special case of the dynamics of systems under a minimal set of c time-independent holonomic constraints (i.e. dependent only on positions) that fix all intra-body distances:

$$\sigma_\alpha(\boldsymbol{r}_N) = 0, \tag{1}$$

where the index α runs over all constraints present in the system and $\boldsymbol{r}_N$ is a generalized vector whose components are the set of all Cartesian coordinates of the N total particles in the system. For fully rigid bodies, the number of constraints c can easily be calculated by noting that the number of spatial degrees of freedom of an n-particle body is $3n$ in 3 dimensions, while only 6 degrees of freedom are necessary to completely specify the position of all components of a rigid body: 3 degrees of freedom for the center of mass of the object and 3 degrees of freedom to specify its orientation with respect to some arbitrary fixed reference frame. There are therefore $c = 3n - 6$ constraint equations for a single rigid body with n point masses. Below, these point masses will be referred to as *atoms* while the body as a whole will be called a *molecule*. A typical constraint equation fixes the distance between atoms i and j in the molecule to be some value, d, i.e.,

$$\sigma(r_{ij}) = \frac{1}{2}\left(r_{ij}^2 - d^2\right) = 0. \tag{2}$$

The equations of motion for the system follow from Hamilton's principle of stationary action, which states that the motion of the system over a fixed time interval is such that the variation of the line integral defining the action $\mathcal{S}$ is zero:

$$\mathcal{S} = \int_{t_1}^{t_2} \mathcal{L}(\boldsymbol{r}_N(t), \dot{\boldsymbol{r}}_N(t))\, dt \tag{3}$$

$$\delta\mathcal{S} = \delta \int_{t_1}^{t_2} \mathcal{L}(\boldsymbol{r}_N(t), \dot{\boldsymbol{r}}_N(t))\, dt = 0, \tag{4}$$

where the Lagrangian $\mathcal{L}$ in the presence of the constraints is written in Cartesian coordinates as

$$\mathcal{L}(\boldsymbol{r}_N, \dot{\boldsymbol{r}}_N) = \sum_{i=1}^{N} \frac{m_i}{2}|\dot{\boldsymbol{r}}_i|^2 - \lambda_\alpha\sigma_\alpha(\boldsymbol{r}_N) - \Phi(\boldsymbol{r}_N), \tag{5}$$

where Φ is the interaction potential. For clarity throughout this paper, the Einstein summation convention will be used for sums over repeated *greek* indices i.e. $\lambda_\alpha\sigma_\alpha \equiv \sum_{\alpha=1}^{c} \lambda_\alpha\sigma_\alpha$, whereas the sum over atom indices will be written explicitly. In Eq. (5), the parameters λ_α are Lagrange multipliers to enforce the distance constraints σ_α. The resulting equations of motion are:

$$\frac{d}{dt}\frac{\partial\mathcal{L}}{\partial\dot{\boldsymbol{r}}_i} = \frac{\partial\mathcal{L}}{\partial\boldsymbol{r}_i} \tag{6}$$

$$m_i\ddot{\boldsymbol{r}}_i = -\lambda_\alpha\frac{\partial\sigma_\alpha}{\partial\boldsymbol{r}_i} - \frac{\partial\Phi}{\partial\boldsymbol{r}_i}. \tag{7}$$

For an elementary discussion of constrained dynamics in the Lagrangian formulation of mechanics, we refer to Ref. 20.

When there are no interactions, such as for a single molecule, the potential $\Phi = 0$ and Eq. (7) becomes

$$m_i\ddot{\boldsymbol{r}}_i = -\lambda_\alpha\frac{\partial\sigma_\alpha}{\partial\boldsymbol{r}_i}. \tag{8}$$

These equations of motion must be supplemented by equations for the c Lagrange multipliers λ_α, which are functions of time. Although the λ_α are not functions of $\boldsymbol{r}_N$ and $\dot{\boldsymbol{r}}_N$ in a mathematical sense, it will be shown below that once the equations are solved they can be expressed in terms of $\boldsymbol{r}_N$ and $\dot{\boldsymbol{r}}_N$. Note that the equations of motion show that even in the absence of an external potential, the motion of the point masses (atoms) making up a rigid body (molecule) are non-trivial due to the emergence of a *constraint force* $-\lambda_\alpha \partial\sigma_\alpha/\partial \boldsymbol{r}_i$.

In fortuitous cases, the time dependence of the Lagrange multipliers is relatively simple and can be solved for by Taylor expansion of the Lagrange multipliers in time t. To evaluate the time derivatives of the multipliers, one can use time derivatives of the initial constraint conditions, which must vanish to all orders. The result is a hierarchy of equations, which, at order k, is linear in the unknown kth time derivatives $\lambda_\alpha^{(k)}$ but depends on the lower order time derivatives $\lambda_\alpha^{(0)}$, $\lambda_\alpha^{(1)}$, $\ldots \lambda_\alpha^{(k-1)}$. In exceptional circumstances, this hierarchy naturally truncates. For example, for a rigid diatomic molecule with a single bond length constraint, one finds that the hierarchy truncates at order $k = 0$, and the Lagrange multiplier is a constant [15]. However this is not the typical case.

Alternatively, since the constraints $\sigma_\alpha(\boldsymbol{r}_N) = 0$ are to be satisfied at all times t, and not just at time zero, their time derivatives are zero at all times. From the first time derivative

$$\dot{\sigma}_\alpha(\boldsymbol{r}_N) = 0,$$

one sees that the initial velocities $\boldsymbol{v}_i = \dot{\boldsymbol{r}}_i$ must obey

$$\sum_i \boldsymbol{v}_i \cdot \frac{\partial \sigma_\alpha}{\partial \boldsymbol{r}_i} = 0, \tag{9}$$

for each constraint condition α. The Lagrange multipliers can be determined by the condition that the second derivatives of all the constraints vanish so that

$$\begin{aligned}
\ddot{\sigma}_\alpha(\boldsymbol{r}_N) &= \sum_i \frac{\partial \sigma_\alpha(\boldsymbol{r}_N)}{\partial \boldsymbol{r}_i} \cdot \ddot{\boldsymbol{r}}_i + \sum_{i,j} \dot{\boldsymbol{r}}_j \cdot \frac{\partial^2 \sigma_\alpha(\boldsymbol{r}_N)}{\partial \boldsymbol{r}_j \partial \boldsymbol{r}_i} \cdot \dot{\boldsymbol{r}}_i \\
&= -\sum_i \frac{\partial \sigma_\alpha(\boldsymbol{r}_N)}{\partial \boldsymbol{r}_i} \cdot \frac{\lambda_\beta}{m_i} \frac{\partial \sigma_\beta(\boldsymbol{r}_N)}{\partial \boldsymbol{r}_i} \\
&\quad + \sum_{i,j} \dot{\boldsymbol{r}}_j \cdot \frac{\partial^2 \sigma_\alpha(\boldsymbol{r}_N)}{\partial \boldsymbol{r}_j \partial \boldsymbol{r}_i} \cdot \dot{\boldsymbol{r}}_i \\
&= 0,
\end{aligned}$$

yielding a linear equation for the Lagrange multipliers that can be solved in matrix form as

$$\lambda_\alpha(t) = \mathbf{Z}^{-1}_{\alpha\beta}(\boldsymbol{r}_N(t)) \mathcal{T}_\beta(\boldsymbol{r}_N(t), \dot{\boldsymbol{r}}_N(t)), \tag{10}$$

where

$$\mathcal{T}_\beta(\boldsymbol{r}_N, \dot{\boldsymbol{r}}_N) = \sum_{i,j} \dot{\boldsymbol{r}}_j \cdot \frac{\partial^2 \sigma_\beta(\boldsymbol{r}_N)}{\partial \boldsymbol{r}_j \partial \boldsymbol{r}_i} \cdot \dot{\boldsymbol{r}}_i \tag{11}$$

$$\mathbf{Z}_{\alpha\beta}(\boldsymbol{r}_N) = \sum_i \frac{1}{m_i} \frac{\partial \sigma_\alpha(\boldsymbol{r}_N)}{\partial \boldsymbol{r}_i} \cdot \frac{\partial \sigma_\beta(\boldsymbol{r}_N)}{\partial \boldsymbol{r}_i}. \tag{12}$$

It may be shown that with λ_α given by Eq. (10), all higher time derivatives of σ_α are automatically zero.

As Eq. (10) shows, in general the Lagrange multipliers are dependent on both the positions $\boldsymbol{r}_N$ and the velocities $\dot{\boldsymbol{r}}_N$ of the particles. To see that this makes the dynamics non-Hamiltonian, the equations of motion can be cast into Hamiltonian-like form using $\boldsymbol{p}_i = m_i \dot{\boldsymbol{r}}_i$, i.e.,

$$\begin{aligned}
\dot{\boldsymbol{r}}_i &= \frac{\boldsymbol{p}_i}{m_i} \\
\dot{\boldsymbol{p}}_i &= -\lambda_\alpha \frac{\partial \sigma_\alpha}{\partial \boldsymbol{r}_i},
\end{aligned} \tag{13}$$

where it is apparent that the forces in the system depend on the momentum through λ in Eq. (10). There exists no Hamiltonian that generates these equations of motion.[21]

Since the underlying dynamics of the system is non-Hamiltonian, the statistical mechanics of the constrained system is potentially more complex. In general, phase-space averages have to be defined with respect to a metric that is invariant to the standard measure of Hamiltonian systems, but $d\boldsymbol{r}_N d\boldsymbol{p}_N$ is not conserved under the dynamics and the standard form of the Liouville equation does not hold [22, 23]. In general, there is a phase-space compressibility factor κ associated with the lack of conservation of the measure that is given by minus the divergence of the flow in phase space. It may be shown that[23, 24]

$$\kappa = -\frac{\partial}{\partial \boldsymbol{r}_i} \cdot \dot{\boldsymbol{r}}_i - \frac{\partial}{\partial \boldsymbol{p}_i} \cdot \dot{\boldsymbol{p}}_i = \frac{d}{dt} \ln \|\mathbf{Z}(\boldsymbol{r}_N)\|,$$

where $\|\mathbf{Z}(\boldsymbol{r}_N)\|$ is the determinant of the matrix $\mathbf{Z}_{\alpha\beta}(\boldsymbol{r}_N)$ defined in Eq. (12). The compressibility factor is related to the invariant phase-space metric $d\mu = \sqrt{g(\boldsymbol{r}_N, \boldsymbol{p}_N, t)} d\boldsymbol{r}_N d\boldsymbol{p}_N$ with[24, 25]

$$\sqrt{g(\boldsymbol{r}_N, \boldsymbol{p}_N, t)} = \|\mathbf{Z}(\boldsymbol{r}_N)\|. \tag{14}$$

Statistical averages are therefore defined for the non-Hamiltonian system as[26, 27]

$$\begin{aligned}
\langle X(\boldsymbol{r}_N, \boldsymbol{p}_N) \rangle &= \frac{1}{Q} \int d\boldsymbol{p}_N d\boldsymbol{r}_N \, \|\mathbf{Z}(\boldsymbol{r}_N)\| \\
&\quad \times X(\boldsymbol{r}_N, \boldsymbol{p}_N) \, \rho(\boldsymbol{r}_N, \boldsymbol{p}_N) \\
&\quad \times \prod_\alpha \delta(\sigma_\alpha(\boldsymbol{r}_N)) \delta\big(\dot{\sigma}_\alpha(\boldsymbol{r}_N, \boldsymbol{p}_N)\big),
\end{aligned} \tag{15}$$

where $\rho(\boldsymbol{r}_N, \boldsymbol{p}_N)$ is the probability density for the unconstrained system and Q is the partition function for the constrained system, given by

$$\begin{aligned}
Q &= \int d\boldsymbol{p}_N d\boldsymbol{r}_N \, \|\mathbf{Z}(\boldsymbol{r}_N)\| \, \rho(\boldsymbol{r}_N, \boldsymbol{p}_N) \\
&\quad \times \prod_\alpha \delta(\sigma_\alpha(\boldsymbol{r}_N)) \delta\left(\dot{\sigma}_\alpha(\boldsymbol{r}_N, \boldsymbol{p}_N)\right).
\end{aligned}$$

Although the invariant metric is non-uniform for many constrained systems, for entirely rigid systems the $\mathbf{Z}(\boldsymbol{r}_N)$ matrix is a function only of the point masses and fixed distances. Hence the term $\|\mathbf{Z}(\boldsymbol{r}_N)\|$ acts as a multiplicative factor which cancels in the averaging process.

B. Free motion of rigid bodies

Although the solution of the dynamics of constrained systems via time-independent holonomic constraints is intellectually appealing and useful in developing a formal statistical mechanics for these systems, it is often difficult to analytically solve for the values of the Lagrange multipliers at arbitrary times. One therefore often resorts to numerical solutions of the multipliers in iterative form, using algorithms such as SHAKE[28]. Such an approach is not really consistent with the principles of DMD, in which a computationally efficient means of calculating event times is one of the great advantages of the method. For fully-constrained, rigid bodies, it is more sensible to apply other, equivalent, approaches, such as the principal axis or quaternion methods, to calculate analytically the evolution of the system in the absence of external forces.

The basic simplification in the dynamics of rigid bodies results from the fact that the general motion of a rigid body can be decomposed into a translation of the center of mass of the body plus a rotation about the center of mass. The orientation of the body relative to its center of mass is described by the relation between the so-called *body frame*, in which a set of axes are held fixed with the body as it moves, and the fixed external *laboratory frame*. The two frames of reference can be connected by an orthogonal transformation, such that the position of an atom i in a rigid body can be written at an arbitrary time t as:

$$\boldsymbol{r}_i(t) = \boldsymbol{R}(t) + \mathbf{A}^\dagger(t)\,\tilde{\boldsymbol{r}}_i, \tag{16}$$

where $\tilde{\boldsymbol{r}}_i$ is the position of atom i in the body frame (which is independent of time), $\boldsymbol{R}(t)$ is the center of mass, and the matrix $\mathbf{A}^\dagger(t)$ is the orthogonal matrix that converts coordinates in the body frame to the laboratory frame. Note that matrix-vector and matrix-matrix multiplication will be implied throughout the paper. The matrix $\mathbf{A}^\dagger(t)$ is the transpose of $\mathbf{A}(t)$, which converts coordinates from the laboratory frame to the body frame at time t. The elements composing the columns of the matrix $\mathbf{A}^\dagger(t)$ are simply the coordinates of the axes in the body frame written in the laboratory frame. Note that Eq. (16) implies that the relative vector $\overline{\boldsymbol{r}}_i(t)$ satisfies

$$\overline{\boldsymbol{r}}_i = \boldsymbol{r}_i - \boldsymbol{R} = \mathbf{A}^\dagger\,\tilde{\boldsymbol{r}}_i, \tag{17}$$

Here as well as below, we have dropped the explicit time dependence for most time dependent quantities with the exception of quantities at time zero or at a time that is integrated over.

One sees that in order to determine the location of different parts of the body in the laboratory frame, the rotation matrix $\mathbf{A}$ must be specified. This matrix satisfies a differential equation that will now be derived and subsequently solved.

Before doing so, it will be useful to restate some properties of rotation matrices and establish some notation to be used below. Formally, a rotation matrix $\mathbf{U}$ is an orthogonal matrix with determinant one and whose its inverse is equal to its transpose $\mathbf{U}^\dagger$. Any rotation can be specified by a rotation axis $\hat{\boldsymbol{n}} = (n_1, n_2, n_3)$ and an angle θ over which to rotate. Here $\hat{\boldsymbol{n}}$ is a unit vector, so that one may also say that any non-unit vector $\theta\hat{\boldsymbol{n}}$ can be used to specify a rotation, where its norm is equal to the angle θ and its direction is equal to the axis $\hat{\boldsymbol{n}}$. According to Rodrigues' formula, the matrix corresponding to this rotation is[20]

$$\mathbf{U}(\theta\hat{\boldsymbol{n}}) = \begin{pmatrix} n_1^2 + \left(n_2^2+n_3^2\right)\cos\theta & n_1 n_2\,(1-\cos\theta) - n_3\sin\theta & n_1 n_3\,(1-\cos\theta) + n_2\sin\theta \\ n_1 n_2\,(1-\cos\theta) + n_3\sin\theta & n_2^2 + \left(n_1^2+n_3^2\right)\cos\theta & n_2 n_3\,(1-\cos\theta) - n_1\sin\theta \\ n_3 n_1\,(1-\cos\theta) - n_2\sin\theta & n_3 n_2\,(1-\cos\theta) + n_1\sin\theta & n_3^2 + \left(n_1^2+n_2^2\right)\cos\theta \end{pmatrix}. \tag{18}$$

The derivation of the differential equation for $\mathbf{A}$ starts by taking the time derivative of Eq. (16), yielding

$$\boldsymbol{v}_i - \boldsymbol{V} = \dot{\mathbf{A}}^\dagger\,\tilde{\boldsymbol{r}}_i = \dot{\mathbf{A}}^\dagger\,\mathbf{A}\,\overline{\boldsymbol{r}}_i. \tag{19}$$

From elementary classical mechanics[20], it is known that this relative velocity can also be written as

$$\boldsymbol{v}_i - \boldsymbol{V} = \boldsymbol{\omega} \times \overline{\boldsymbol{r}}_i, \tag{20}$$

where $\boldsymbol{\omega}$ is the angular velocity vector in the lab frame. Since both Eq. (19) and Eq. (20) are true for any vector $\overline{\boldsymbol{r}}_i$, it follows that $\dot{\mathbf{A}}^\dagger\,\mathbf{A}$ is the matrix representation of a cross product with the angular velocity $\boldsymbol{\omega}$, i.e.,

$$\dot{\mathbf{A}}^\dagger\,\mathbf{A} = \begin{pmatrix} 0 & -\omega_3 & \omega_2 \\ \omega_3 & 0 & -\omega_1 \\ -\omega_2 & \omega_1 & 0 \end{pmatrix} \equiv \mathbf{W}(\boldsymbol{\omega}). \tag{21}$$

Multiplying Eq. (21) on the right with $\mathbf{A}^\dagger$ and taking the transpose on both sides (note that $\mathbf{W}$ is antisymmetric) yields

$$\dot{\mathbf{A}} = -\mathbf{A}\,\mathbf{W}(\boldsymbol{\omega}). \tag{22}$$

This equation involves the angular velocity in the laboratory frame, but the rotational equations of motion are more easily solved in the body frame. The angular velocity vector transforms to the body frame according to

$$\tilde{\boldsymbol{\omega}} = \mathbf{A}\,\boldsymbol{\omega}. \tag{23}$$

For any rotation $\mathbf{A}$ and vector $\boldsymbol{x}$ one has $\mathbf{W}(\mathbf{A}\,\boldsymbol{x}) = \mathbf{A}\,\mathbf{W}(\boldsymbol{x})\,\mathbf{A}^\dagger$, hence one can write

$$\mathbf{W}(\boldsymbol{\omega}) = \mathbf{W}(\mathbf{A}^\dagger\,\tilde{\boldsymbol{\omega}}) = \mathbf{A}^\dagger\,\mathbf{W}(\tilde{\boldsymbol{\omega}})\,\mathbf{A}. \tag{24}$$

Substituting Eq. (24) into Eq. (22) yields the differential equation for $\mathbf{A}$:

$$\dot{\mathbf{A}} = -\mathbf{W}(\tilde{\boldsymbol{\omega}})\,\mathbf{A}. \tag{25}$$

Although the choice of body frame is arbitrary, perhaps the most convenient choice of axes for the body are the so-called principal axes in which the moment of inertia tensor $\tilde{\mathbf{I}}$ is diagonal, i.e., $\tilde{\mathbf{I}} = \mathrm{diag}(I_1, I_2, I_3)$. Choosing this reference frame as the body frame, the representation of the components of the angular momentum $\tilde{\boldsymbol{L}}$ is

$$\tilde{\boldsymbol{L}} = \tilde{\mathbf{I}}\,\tilde{\boldsymbol{\omega}} = \begin{pmatrix} I_1\tilde{\omega}_1 \\ I_2\tilde{\omega}_2 \\ I_3\tilde{\omega}_3 \end{pmatrix}, \tag{26}$$

where I_k and $\tilde{\omega}_k$ are the principal moments of inertia and principal components of the angular velocity.

The time dependence of the principal components of the angular velocity may be obtained from the standard expression for the torque in the laboratory frame:

$$\begin{aligned} \boldsymbol{\tau} = \dot{\boldsymbol{L}} &= \dot{\mathbf{A}}^\dagger\,\tilde{\boldsymbol{L}} + \mathbf{A}^\dagger\,\dot{\tilde{\boldsymbol{L}}} \\ &= \mathbf{A}^\dagger\,\left[\tilde{\boldsymbol{\omega}} \times \tilde{\boldsymbol{L}} + \dot{\tilde{\boldsymbol{L}}}\right]. \end{aligned} \tag{27}$$

where Eq. (25) was used in the last equality. Transforming Eq. (27) to the principal axis frame gives Euler's equations of motion for a rigid body

$$\begin{aligned} I_1\dot{\tilde{\omega}}_1 - \tilde{\omega}_2\tilde{\omega}_3(I_2 - I_3) &= \tilde{\tau}_1 \\ I_2\dot{\tilde{\omega}}_2 - \tilde{\omega}_1\tilde{\omega}_3(I_3 - I_1) &= \tilde{\tau}_2 \\ I_3\dot{\tilde{\omega}}_3 - \tilde{\omega}_1\tilde{\omega}_2(I_1 - I_2) &= \tilde{\tau}_3, \end{aligned} \tag{28}$$

where $\tilde{\tau}_k$ are the components of the torque $\tilde{\boldsymbol{\tau}} = \mathbf{A}\,\boldsymbol{\tau}$ in the body frame. Note that even in the absence of any torque, the principal components of the angular velocity are in general time dependent.

Once the angular velocity $\tilde{\boldsymbol{\omega}}$ is known, it can be substituted into Eq. (25) for the matrix $\mathbf{A}$. The general solution of Eq. (25) is of the form

$$\mathbf{A} = \mathbf{P}\,\mathbf{A}(0). \tag{29}$$

where $\mathbf{P}$ is a rotation matrix itself which 'propagates' the orientation $\mathbf{A}(0)$ to the orientation at time t. $\mathbf{P}$ satisfies the same equation (25) as $\mathbf{A}$, but with initial condition $\mathbf{P}(0) = \mathbb{1}$. By integrating this equation, one can obtain an expression for $\mathbf{P}$. At first glance, it may seem that $\mathbf{P}$ can only be written as a formal expression containing a time-ordered exponential. However, for the torque-free case $\boldsymbol{\tau} = 0$, the conservation of angular momentum and energy and the orthogonality of the matrix $\mathbf{P}$ can be used to derive the following explicit expression[29] (implicitly also found in Ref. 14):

$$\mathbf{P} = \mathbf{T}_1\,\mathbf{T}_2. \tag{30}$$

Here $\mathbf{T}_1$ and $\mathbf{T}_2$ are two rotation matrices. The matrix $\mathbf{T}_1$ rotates $\tilde{\boldsymbol{L}}(0)$ to $\tilde{\boldsymbol{L}}$ and can be written as

$$\mathbf{T}_1 = \begin{pmatrix} c_1c_2 - s_1s_2c_3 & c_1s_2 + s_1c_2c_3 & s_1s_3 \\ -s_1c_2 - c_1s_2c_3 & -s_1s_2 + c_1c_2c_3 & c_1s_3 \\ s_2s_3 & -c_2s_3 & c_3 \end{pmatrix}, \tag{31}$$

where

$$s_1 = \frac{\tilde{L}_1}{\tilde{L}_\perp} \qquad c_1 = \frac{\tilde{L}_2}{\tilde{L}_\perp} \tag{32}$$

$$s_2 = -\frac{\tilde{L}_1(0)}{\tilde{L}_\perp(0)} \qquad c_2 = \frac{\tilde{L}_2(0)}{\tilde{L}_\perp(0)} \tag{33}$$

$$s_3 = \frac{\tilde{L}_\perp\tilde{L}_3(0) - \tilde{L}_3\tilde{L}_\perp(0)}{L^2} \quad c_3 = \frac{\tilde{L}_\perp\tilde{L}_\perp(0) + \tilde{L}_3\tilde{L}_3(0)}{L^2} \tag{34}$$

and $\tilde{L}_\perp = \sqrt{\tilde{L}_1^2 + \tilde{L}_2^2}$ while $L = |\tilde{\boldsymbol{L}}|$.

The matrix $\mathbf{T}_2$ can be expressed, using the notation in Eq. (18), as

$$\mathbf{T}_2 = \mathbf{U}(-\psi L^{-1}\tilde{\boldsymbol{L}}(0)), \tag{35}$$

where the angle ψ is given by

$$\psi = \int_0^t dt'\,\Omega(t'), \tag{36}$$

with

$$\Omega = L\frac{I_1\tilde{\omega}_1^2 + I_2\tilde{\omega}_2^2}{\tilde{L}_\perp^2}. \tag{37}$$

The angle ψ can be interpreted as an angle over which the body rotates. If the body rotates one way, the laboratory frame as seen from the body frame rotates in the opposite way, which explains the minus sign in Eq. (35). For the derivation of Eqs. (30)-(37) we refer to Ref. 29. Similar equations, but in a special reference frame, can be found in Ref. 14.

In the following, the solution of Eq. (28) with $\boldsymbol{\tau} = 0$ for bodies of differing degrees of symmetry will be analyzed and then used to obtain explicit expressions for the matrix $\mathbf{P}$ as a function of time and of the initial angular velocity in the body frame $\tilde{\boldsymbol{\omega}}(0)$.

Case 1. Spherical rotor

For the case of a spherical rotor in which all three moments of inertia are equal, $I_1 = I_2 = I_3$, the form of

the Euler equations (28) is particularly simple: $I_1\dot{\tilde{\omega}}_j = 0$. It is therefore clear that all components of the angular velocity in the body frame are conserved, as are those of the angular momentum. As a result, $\mathbf{T}_1$ in Eq. (31) is equal to the identity matrix. A second consequence is that Ω in Eq. (37) is constant, so that $\psi = \Omega\, t$ where Ω may be rewritten, using $I_1 = I_2 = I_3$, as $\Omega = L/I_1 = |\boldsymbol{\omega}|$. Therefore Eqs. (30) and (35) give

$$\mathbf{P} = \mathbf{U}(-\boldsymbol{\omega} t), \tag{38}$$

corresponding to a rotation by an angle of $-\Omega t$ around the axis $\boldsymbol{\omega}/\Omega$.

Case 2. Symmetric top

For the case of a symmetric top for which $I_1 = I_2$, one can solve the Euler equations (28) in terms of simple sines and cosines, since Eq. (28) becomes

$$\begin{aligned} \dot{\tilde{\omega}}_1 &= \omega_p\, \tilde{\omega}_2 \\ \dot{\tilde{\omega}}_2 &= -\omega_p\, \tilde{\omega}_1 \\ \dot{\tilde{\omega}}_3 &= 0, \end{aligned} \tag{39}$$

where $\omega_p = \left(1 - \frac{I_3}{I_1}\right)\tilde{\omega}_3(0)$ is the precession frequency. The full solution of the Euler equations (39) is given by

$$\tilde{\boldsymbol{\omega}} = \begin{pmatrix} \tilde{\omega}_1(0)\cos\omega_p t + \tilde{\omega}_2(0)\sin\omega_p t \\ -\tilde{\omega}_1(0)\sin\omega_p t + \tilde{\omega}_2(0)\cos\omega_p t \\ \tilde{\omega}_3(0) \end{pmatrix}. \tag{40}$$

Using Eq. (40) and the fact that $\tilde{L}_\perp$ and $\tilde{L}_3$ are conserved in this case, one can easily show that $\mathbf{T}_1$ is given by

$$\mathbf{T}_1 = \begin{pmatrix} \cos\omega_p t & \sin\omega_p t & 0 \\ -\sin\omega_p t & \cos\omega_p t & 0 \\ 0 & 0 & 1 \end{pmatrix} = \mathbf{U}(-\omega_p t\hat{\boldsymbol{z}}). \tag{41}$$

and one can determine Ω from Eq. (37):

$$\Omega = \frac{L[I_1\tilde{\omega}_1^2(0) + I_1\tilde{\omega}_2^2(0)]}{I_1^2\tilde{\omega}_1^2(0) + I_1^2\tilde{\omega}_2^2(0)} = \frac{L}{I_1}. \tag{42}$$

This is a constant so that $\psi = \frac{L}{I_1}t$. Thus

$$\mathbf{T}_2 = \mathbf{U}\left(-\frac{\tilde{\boldsymbol{L}}(0)t}{I_1}\right), \tag{43}$$

and one gets from Eq. (30):

$$\mathbf{P} = \mathbf{U}(-\omega_p t\hat{\boldsymbol{z}})\,\mathbf{U}\left(-\frac{\tilde{\boldsymbol{L}}(0)t}{I_1}\right). \tag{44}$$

Case 3. Asymmetric body

If all the principal moments of inertia are distinct, the time dependence of the angular velocity $\tilde{\boldsymbol{\omega}}$ involves elliptic functions[20]. While this may seem complicated, efficient standard numerical routines exist to evaluate these functions[30, 31, 32, 33, 34]. More challenging is the evaluation of the matrix $\mathbf{P}$. While its exact solution has been known for more than 170 years[9, 10], it is formulated--even in more recent texts[11, 12]--in terms of undetermined constants and using complex algebra, which hinders its straightforward implementation in a numerical simulation. It is surprisingly difficult to find an explicit formula in the literature for the matrix $\mathbf{P}$ as a function of the initial conditions, which is the form needed in DMD simulations. For this reason, the explicit general solution for $\mathbf{P}$ will briefly be presented here in terms of general initial conditions. The details of the derivation can be found elsewhere[29].

Following Jacobi[10], it is useful to adopt the convention that I_2 is the moment of inertia intermediate in magnitude (i.e., either $I_1 < I_2 < I_3$ or $I_1 > I_2 > I_3$) and one chooses the overall ordering of magnitudes, such that:

$$\begin{aligned} I_1 > I_2 > I_3 \;\; &\text{if } E_R > \frac{L^2}{2I_2} \\ I_1 < I_2 < I_3 \;\; &\text{if } E_R < \frac{L^2}{2I_2}, \end{aligned} \tag{45}$$

where E_R is the rotational kinetic energy $E_R = \frac{1}{2}(I_1\tilde{\omega}_1^2 + \tilde{\omega}_2^2 + I_3\tilde{\omega}_3^2)$ and L is the norm of the angular momentum $L = (I_1^2\tilde{\omega}_1^2 + I_2^2\tilde{\omega}_2^2 + I_3^2\tilde{\omega}_3^2)^{1/2}$. Without this convention some quantities defined below would be complex valued, which is numerically inconvenient and inefficient. Note that in a simulation molecules will often be assigned a specific set of physical inertial moments with fixed order, i.e. not depending on the particular values of E_R and L. A simple way to nevertheless adopt the convention in Eq. (45) is to introduce internal variables $\tilde{\boldsymbol{\omega}}_{int} = \mathbf{T}_{int}\tilde{\boldsymbol{\omega}}$, $\tilde{\mathbf{I}}_{int} = \mathbf{T}_{int}\tilde{\mathbf{I}}\mathbf{T}_{int}$ and $\mathbf{A}_{int} = \mathbf{T}_{int}\tilde{\mathbf{A}}\mathbf{T}_{int}$ which differ when necessary from the physical ones by a rotation given by the rotation matrix

$$\mathbf{T}_{int} = \begin{pmatrix} 0 & 0 & 1 \\ 0 & -1 & 0 \\ 1 & 0 & 0 \end{pmatrix}. \tag{46}$$

This matrix interchanges the x and z directions and reversed the y direction, and is equal to its inverse.

The Euler equations (28) can be solved because there are two conserved quantities E and L^2 which allow $\tilde{\omega}_1$ and $\tilde{\omega}_3$ to be expressed in terms of $\tilde{\omega}_2$, at least up to a sign which the quadratic conserved quantities cannot prescribe. In this way the three coupled equations (28) are reduced to a single ordinary differential equation for $d\tilde{\omega}_2/dt$, from which t can be solved as an integral over $\tilde{\omega}_2$: This is an incomplete elliptic integral of the first kind[30, 31]. To get $\tilde{\omega}_2$ as a function of t, one needs its

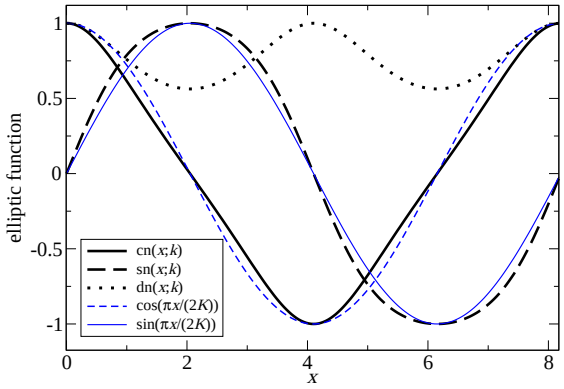

FIG. 1: Example of the elliptic functions cn (solid line), sn (bold dashed line), dn (dotted line) for $m = 0.465$ ($K = 2.05$, $K' = 1.72$, $q = 0.071$). Also plotted are the cosine (short dashed line) and sine (thin short dashed line) with the same period, for comparison.

inverse, which is the elliptic function sn[30, 31]. Without giving further details, the solution of the Euler equations is given by[10, 11, 13, 29]

$$\tilde{\boldsymbol{\omega}} = \begin{pmatrix} \omega_{1m}\,\mathrm{cn}(\omega_p t + \varepsilon|m) \\ \omega_{2m}\,\mathrm{sn}(\omega_p t + \varepsilon|m) \\ \omega_{3m}\,\mathrm{dn}(\omega_p t + \varepsilon|m) \end{pmatrix}. \tag{47}$$

Here cn and dn are also elliptic functions[30, 31, 35], while the ω_{im} are the extreme (maximum or minimum) values of the ω_i and are given by

$$\begin{aligned} \omega_{1m} &= \mathrm{sgn}(\tilde{\omega}_1(0))\sqrt{\frac{L^2 - 2I_3E_R}{I_1(I_1 - I_3)}} \\ \omega_{2m} &= -\,\mathrm{sgn}(\tilde{\omega}_1(0))\sqrt{\frac{L^2 - 2I_3E_R}{I_2(I_2 - I_3)}} \\ \omega_{3m} &= \mathrm{sgn}(\tilde{\omega}_3(0))\sqrt{\frac{L^2 - 2I_1E_R}{I_3(I_3 - I_1)}}, \end{aligned} \tag{48}$$

where $\mathrm{sgn}(x)$ is the sign of x. Furthermore, in Eq. (47) the *precession frequency* ω_p is given by

$$\omega_p = \mathrm{sgn}(I_2 - I_3)\,\mathrm{sgn}(\tilde{\omega}_3(0))\sqrt{\frac{(L^2 - 2I_1E_R)(I_3 - I_2)}{I_1I_2I_3}}. \tag{49}$$

The elliptic functions are periodic functions of their first argument, and look very similar to the sine, cosine and constant function. They furthermore depend on the *elliptic parameter* m (or elliptic modulus $\sqrt{m}$), which determines how closely the elliptic functions resemble their trigonometric counterparts, and which is given by

$$m = \frac{(I_1 - I_2)(L^2 - 2I_3E_R)}{(I_3 - I_2)(L^2 - 2I_1E_R)}. \tag{50}$$

By matching the values of $\tilde{\omega}_2$ at time zero, one can determine the integration constant ε:

$$\varepsilon = F\big(\tilde{\omega}_{20}/\tilde{\omega}_{2m}|m\big), \tag{51}$$

where F is the incomplete elliptic integral of the first kind[30, 31]

$$F(y|m) = \int_0^y \frac{dx}{\sqrt{(1-x^2)(1-mx^2)}}. \tag{52}$$

In fact, $\mathrm{sn}(x|m)$ is simply the inverse of this function. As a result of the ordering convention in Eq. (45), the parameter m in Eq. (50) is guaranteed to be less than one, which is required in order that $F(y|m)$ in Eq. (52) not be complex-valued.

Three more numbers can be derived from the elliptic parameter m which play an important role in the elliptic functions. These are the *quarter-period* $K = F(1|m)$, the *complementary quarter-period* $K' = F(1|1-m)$ and the *nome* $q = \exp(-\pi K'/K)$, which is the parameter in various series expansions.

The period of the elliptic functions cn and sn is equal to $4K$, while that of dn is $2K$. These elliptic functions have the following Fourier series[30, 31]:

$$\mathrm{cn}(x|m) = \frac{2\pi}{\sqrt{m}K}\sum_{n=0}^{\infty}\frac{q^{n+1/2}}{1+q^{2n+1}}\cos\frac{(2n+1)\pi x}{2K} \tag{53}$$

$$\mathrm{sn}(x|m) = \frac{2\pi}{\sqrt{m}K}\sum_{n=0}^{\infty}\frac{q^{n+1/2}}{1-q^{2n+1}}\sin\frac{(2n+1)\pi x}{2K} \tag{54}$$

$$\mathrm{dn}(x|m) = \frac{\pi}{2K} + \frac{2\pi}{K}\sum_{n=1}^{\infty}\frac{q^{n}}{1-q^{2n}}\cos\frac{n\pi x}{K}. \tag{55}$$

Note that the right-hand side of Eqs. (53)-(55) depends on m through $K = F(1|m)$ and $q = \exp[-\pi F(1|1-m)/K]$. For $m = 0$, one gets $q = 0$ and cn, sn and dn reduce to cos, sin and 1, respectively. The constancy of $\mathrm{dn}(x|m=0)$ is reminiscent of the conservation of $\tilde{\omega}_3$ in the case of the symmetric top, and, indeed, for $I_1 = I_2$, $m = 0$ according to Eq. (50).

Typical values for q are quite small, hence often the elliptic function sn, cn and dn resemble the cos, sin and a constant function with value one (as e.g. in Fig. 1). For small values of q, the series expressions for the elliptic functions converge quickly (although this is not the best way to compute the elliptic functions[30, 31, 32, 33, 34]).

Having given the solutions of the Euler equations, we now turn to the solution of Eq. (25) as given by Eqs. (29)-(37). The expression on the right-hand side of Eq. (37) isnot a constant in this case but involves elliptic functions. Despite this difficulty, the integral can still be performed using some properties of elliptic functions, with the result[29]

$$\psi(t) = A_1 + A_2 t - \phi(t). \tag{56}$$

The constants A_1, A_2 and the periodic function $\phi(t)$ can be expressed using the theta function $H(u|m)$[10, 30, 31]

as

$$\phi(t) = \arg H\big(\omega_p t + \varepsilon - \mathrm{i}\eta|m\big) \tag{57}$$

$$A_1 = \phi(0) = \arg H(\varepsilon - \mathrm{i}\eta|m) \tag{58}$$

$$A_2 = \frac{L}{I_1} + \omega_p \frac{d\log H(\mathrm{i}\eta|m)}{d\eta}, \tag{59}$$

where we have used the definition

$$\eta = \mathrm{sgn}(\tilde{\omega}_{30})K' - F\left(\frac{I_3\omega_{3m}}{L}\Big|1-m\right). \tag{60}$$

The equations (57)-(59) involve complex values which are not convenient for numerical evaluation. Using the known series expansions of the theta function H and its logarithmic derivative[30, 31] in terms of the nome q, these equations may be rewritten in a purely real form. In fact, one readily obtains the sine and cosine of ψ, which are all that is needed in Eqs. (18) and (35),

$$\begin{aligned}\cos\psi(t) &= \frac{h_r(t)\cos(A_1+A_2t) + h_i(t)\sin(A_1+A_2t)}{\sqrt{h_r^2(t)+h_i^2(t)}}\\ \sin\psi(t) &= \frac{h_r(t)\sin(A_1+A_2t) - h_i(t)\cos(A_1+A_2t)}{\sqrt{h_r^2(t)+h_i^2(t)}}.\end{aligned} \tag{61}$$

with

$$\begin{aligned}h_r(t) &= \mathrm{Re}\, H(\omega_p t + \varepsilon - \mathrm{i}\eta|m)\\ &= 2q^{1/4}\sum_{n=0}^{\infty}(-1)^n q^{n(n+1)}\cosh\frac{(2n+1)\pi\eta}{2K}\\ &\qquad\times\sin\frac{(2n+1)\pi(\omega_p t+\varepsilon)}{2K}\end{aligned} \tag{62}$$

$$\begin{aligned}h_i(t) &= \mathrm{Im}\, H\big(\omega_p t + \varepsilon - \mathrm{i}\eta|m\big)\\ &= -2q^{1/4}\sum_{n=0}^{\infty}(-1)^n q^{n(n+1)}\sinh\frac{(2n+1)\pi\eta}{2K}\\ &\qquad\times\cos\frac{(2n+1)\pi(\omega_p t+\varepsilon)}{2K},\end{aligned} \tag{63}$$

while the constant A_1 is

$$A_1 = \arctan[h_i(0)/h_r(0)] + n\pi, \tag{64}$$

where $n = 0$ if $h_r(0) > 0$, $n = 1$ if $h_r(0) < 0$ and $h_i(0) > 0$, and $n = -1$ if $h_r(0) < 0$ and $h_i(0) < 0$. Finally, the constant A_2 is given by[30, 31]

$$A_2 = \frac{L}{I_1} + \frac{\pi\omega_p}{2K}\left[\frac{\xi+1}{\xi-1} - 2\sum_{n=1}^{\infty}\frac{q^{2n}(\xi^n - \xi^{-n})}{1-q^{2n}}\right], \tag{65}$$

where $\xi = \exp(\pi\eta/K)$. The series expansion in q in Eq. (65) convergences for $\xi q^2 < 1$. Because $-K' < \eta < K'$ (cf. Eq. (60)), one has $\xi q^2 \le q < 1$, and the series always converges. Since q is typically small, the convergence is rarely very slow (e.g. for convergence up to relative order δ one needs $O(\log\delta/\log q)$ terms). Note that since the constants A_1 and A_2 depend only on the initial angular velocities, they only need to be calculated once at the beginning of the motion of a free rigid body. On the other hand, the series expansions in Eqs. (62) and (63), which have to be evaluated any time the positions are desired, have extremely fast convergence due to the $q^{n(n+1)}$ appearing in these expressions (for example, unless $m \gtrsim 0.95$, the series converges up to $O(10^{-15})$ occurs taking only three terms).

There are efficient routines to calculate the functions cn, sn dn and F, see e.g. Refs. 30, 31, 32, 33, 34, and the series in Eqs. (62), (63) and (65) converge, the former two quite rapidly in fact. Therefore, despite an apparent preference in the literature for conventional numerical integration of the equations of motion via many successive small time steps even for torque-free cases, the analytical solution can be used to calculate the same quantities in a computationally more efficient manner requiring only the evaluation of special functions. The gain in efficiency should be especially pronounced in applications in which many evaluations at various times could be needed, such as in the root searches in discontinuous molecular dynamics (see below).

III. DETECTION OF INTERACTION EVENTS

A. Calculation of interaction events

If the interaction potential between atoms i and j is assumed to be discontinuous, say of the form

$$\Phi(|\boldsymbol{r}_i - \boldsymbol{r}_j|) = \begin{cases}\Phi_0 & \text{if } |\boldsymbol{r}_i - \boldsymbol{r}_j| \le d\\ \Phi_1 & \text{if } |\boldsymbol{r}_i - \boldsymbol{r}_j| > d,\end{cases} \tag{66}$$

then rigid molecules interacting via this potential evolve freely until there is a change in the potential energy of the system and an *interaction event* or *collision event* occurs. The time at which an event occurs is governed by a collision indicator function $f_{ij} = |\boldsymbol{r}_j - \boldsymbol{r}_i|^2 - d^2$ defined such that at time t_c, $f_{ij}(t_c) = 0$. Here, the time dependence of $\boldsymbol{r}_j$ and $\boldsymbol{r}_i$ can be obtained using the results of Sec. II.

The simplest example of this kind of system consists of two hard spheres of diameter d located at positions $\boldsymbol{r}_j$ and $\boldsymbol{r}_i$. If two spheres are approaching, when they get to a distance d from one another, the potential energy would change from Φ_1 to $\Phi_0 = \infty$ if they kept approaching one another. As this eventually would lead to a violation of energy conservation, the spheres bounce off one another in a *hard-core collision* at time t_c, where t_c is determined by the criterion $f_{ij}(t_c) = |\boldsymbol{r}_j(t_c) - \boldsymbol{r}_i(t_c)|^2 - d^2 = 0$, i.e. by the zeros of the collision indicator function. Another kind of interaction event, with Φ_0 and Φ_1 finite, will be called a *square-well collision* because the potential then has a square well shape.

To find the times at which collisions take place, the zeros of the collision indicator functions must be deter-

mined, which generally has to be done numerically. The calculation of the collision times of non-penetrating rigid objects is an important aspect of manipulating robotic bodies, and is also an important element of creating realistic animation sequences. As a result, many algorithms have been proposed in these contexts to facilitate the event time search[36, 37].

The search for the earliest collision event time can be facilitated using screening strategies to decide when rigid bodies may overlap[36, 37]. Usually, these involve placing the bodies in bounding boxes and using an efficient method to determine when bounding boxes intersect. The simplest way to do this in a simulation of rigid molecules is to place each molecule in the smallest sphere around its center of mass containing all components of the molecule[15]. The position of the sphere is determined by the motion of the center of mass, while any change in orientation of the rigid molecule occurs within the sphere. Collisions between rigid molecules can therefore only occur when their encompassing spheres overlap, and the time at which this occurs can be calculated analytically for any pair of molecules. This time serves as a useful point to begin a more detailed search for collision events (see below). Similarly, one can also calculate the time at which the spheres no longer overlap, and use these event times to bracket a possible root of the collision indicator function. It is crucial to make the time bracketing as tight as possible in any implementation of DMD with numerical root searches because the length of the time bracketing interval determines the required number of evaluations of the positions and velocities of the atoms, and therefore plays a significant role in the efficiency of the overall procedure.

The simplest reliable and reasonably efficient means of detecting a root is to perform a *grid search* that looks for changes in sign of f_{ij}, i.e., one looks at $f_{ij}(t + n\Delta t)$ and $f_{ij}(t+(n+1)\Delta t)$ for successive n. The time points $t+n\Delta t$ will be called the *grid points*. When a time interval in between two grid points is found in which a sign change of f_{ij} occurs, the Newton-Raphson algorithm[32] can be called to numerically determine the root with arbitrary accuracy. Since the Newton-Raphson method requires the calculation of first time derivatives, one must also calculate, for any time t, the derivative $df_{ij}/dt = 2\boldsymbol{r}_{ij}\cdot\boldsymbol{v}_{ij}$, where the notation $\boldsymbol{r}_{ij} = \boldsymbol{r}_j - \boldsymbol{r}_i$ and $\boldsymbol{v}_{ij} = \boldsymbol{v}_j - \boldsymbol{v}_i$ has been used. Such time derivatives are readily evaluated using Eqs. (16) and (19).

Unfortunately, while the Newton-Raphson method is a very efficient algorithm for finding roots, it can be somewhat unstable when one is searching for the roots of an oscillatory function. For translating and rotating rigid molecules, the collision indicator function is indeed oscillatory due to the periodic motion of the relative orientation of two colliding bodies. It is particularly easy to miss so-called *grazing collisions* when the grid search interval Δt is too large, in which case the indicator function is positive in two consecutive points of the grid search, yet nonetheless "dips" below zero in the grid interval. It is important that no roots are missed, for a missed root can lead to a different, even infinite energy (but see Sec. V below). To reduce the frequency of missing grazing collisions to zero, a vanishingly small grid interval Δt would be required. Of course such a scheme is not practical, and one must balance the likelihood of missing events with practical considerations since several collision indicator functions need to be evaluated at each point of the grid. Clearly the efficiency of the root search algorithm significantly depends on the magnitude of grid interval.

To save computation time, a coarser grid can be utilized if a means of handling grazing collisions is implemented. Since the collision indicator function has a local extremum (maximum or minimum, depending on whether $|\boldsymbol{r}_i - \boldsymbol{r}_j|^2$ is initially smaller or larger than d^2) at some time near the time of a grazing collision, a reasonable strategy to find these kind of collision events is to determine the extremum of the indicator function in cases in which the indicator function f_{ij} itself does not change sign on the interval but its derivative df_{ij}/dt does. Furthermore, since the indicator function at the grid points near a grazing collision is typically small, it is fruitful to search only for extrema when the indicator function at one of the grid points lies below some threshold value[38]. To find the local extrema of the indicator function, any simple routine of locating the extrema of a non-linear function can be utilized. For example, Brent's minimization method[32, 39], which is based on a parabolic interpolation of the function, is a good choice for sufficiently smooth one-dimensional functions. Once the extremum is found, it is a simple matter to decide whether or not a real collision exists by checking the sign of f_{ij}.

Once the root has been bracketed (either through a sign change of f_{ij} during the grid search or after searching for an extremum), one can simply use the Newton-Raphson algorithm to find the root to desired accuracy, typically within only a few iterations. The time value returned by the Newton-Raphson routine needs to be in the bracketed interval and $df_{ij}/dt < 0$ if f_{ij} was initially positive and $df_{ij}/dt > 0$ if it was initially negative. If those criteria are not satisfied, the Newton-Raphson algorithm has clearly failed and a less efficient but more reliable method is needed to track down the root. For example, the Van Wijngaarden-Dekker-Brent method[32, 39], which combines bisection and quadratic interpolation, is guaranteed to converge if the function is known to have a root in the interval under analysis.

B. Scheduling events

In the previous section is was shown how to determine the time t_{ij} at which two atoms i and j collide under the assumption that there is no other earlier collision. This we will call a *possible collision event*. In a DMD simulation, once the possible collision events at times t_{ij} have been computed for all possible collision pairs i and j, the earliest event $t^*_{i^*j^*} = \min_{ij} t_{ij}$ should be selected. After

the collision event between atoms i^* and j^* has been executed (according to the rules derived in the next section), the next earliest collision should be performed. However, because the velocities of atoms of the molecules involved in the collision have changed, the previously computed collision times involving these molecules are no longer valid. The next event in the sequence can be determined and performed only after these collision times have been recomputed.

This process describes the basic strategy of DMD, which without further improvements would be needlessly inefficient. For if M is the number of possible collision events, finding the earliest time would require $O(M)$ checks, and $M = O(N^2)$, while the number of invalidated collisions that have to be recomputed after each collision would be $O(N)$. Since the number of collisions in the system per unit of physical time also grows with N, the cost of a simulation for a given physical time would be $O(N^2)$ for the computation of collision times and $O(N^3)$ for finding the first collision event[40]. Fortunately, there are ways to significantly reduce this computational cost[1, 5, 41, 42, 43, 44, 45]. The first technique, also used in molecular dynamics simulations of systems interacting with continuous potentials, reduces the number of possible collision times that have to be computed by employing a *cell division* of the system[1]. Note that while the times of certain interaction events (e.g. involving only the molecule's center of mass) can be expressed in analytical form and thus computed very efficiently, the atom-atom interactions have, in general, an orientational dependence and the possible collision time has to be found by means of a numerical root search as explained in the previous section. As a consequence, the most time consuming task in a DMD simulation with rigid bodies is the numerical root search for the collision times. One can however minimize the required number of collision time computations by dividing the system into a cell structure and sorting all molecules into these cells according to the positions of their centers of mass. Each cell has a diameter of at least the largest "interaction diameter" of a molecule as measured from its center of mass. As a result, molecules can only collide if they are in the same cell or in an adjacent cell, so the number of collision events to determine and to recompute after a collision is much smaller. In this technique, the sorting of molecules into cells is only done initially, while the sorting is dynamically updated by introducing a *cell-crossing event* for each molecule that is also stored[5, 42]. Since the center of mass of a molecule performs linear motion between collision events, one can express its cell-crossing time analytically and therefore the numerical computation of that time is very fast.

The second technique reduces the cost of finding the earliest event time. It consists of storing possible collision and cell-crossing events in a time-ordered structure called a *binary tree*. For details we refer to Refs. 5 and 42 (alternative event scheduling algorithms exist[43, 44] but it is not clear which technique is generally the most efficient[45].)

Finally, a third standard technique is to update the molecules' positions and velocities only at collisions (and possibly upon their crossing the periodic boundaries), while storing the time of their last collision as a property of the molecule called its *local clock*[41]. Whenever needed, the positions and velocities at later times can be determined from the exact solution of force-free and torque-free motion of the previous Sec. II.

The use of cell divisions, a binary event tree to manage the events, and local clocks is a standard practice in DMD simulations and largely improves the simulation's efficiency[5]. To see this, note that in each step of the simulation one picks the earliest event from the tree, which scales as $O(\log N)$ for randomly balanced trees[5, 42]. If it is a cell-collision event, it is then performed and subsequently $O(1)$ collisions and cell crossings are recomputed and added to the event tree ($\propto O(\log N)$). If it is a crossing event, the corresponding molecule is put in its new cell, new possible collision and crossing events are computed ($(O(1))$ and added to the tree ($O(\log N)$). Then the program progresses to the next event. Since still $O(N)$ real events take place per unit of physical time, one sees that using these techniques, the computational cost per unit of physical time due to the computation of possible collisions and cell crossing times scales as $O(N)$ instead of $O(N^2)$, while the cost due to the event scheduling is $O(N \log N)$ per unit of physical time instead of $O(N^3)$ -- a huge reduction.

Contrary to what their scaling may suggest, one often finds that the cost of the computation of collision times greatly dominates the scheduling cost for finite N. This is due to fact that the computations of many of the collision times requires numerical root searches, although some can, and should, be done analytically. Thus, to gain further computational improvements, one has to improve upon the efficiency of the numerical search for collision event times. A non-standard time-saving technique that we have developed for this purpose is to use *virtual collision events*. In this case, the grid search (see Sec. III) for a possible collision time of atoms i and j is carried out only over a fixed small number of grid points, thus limiting the scope of the root search to a small search interval. If no collisions are detected in this search interval, a virtual collision event is scheduled in the binary event tree, much as if it were a possible future collision at the time of the last grid point that was investigated. If the point at which the grid search is curtailed is rather far in the future, it is likely this virtual event will not be executed because the atoms i and j probably will have collided with other atoms beforehand. Thus, computational work has been saved by stopping the grid search after a few grid points. Every now and then however, atoms i and j will not have collided with other atoms at the time at which the grid search was stopped. In this case, the virtual collision event in the tree is executed, which entails continuing the root search from the point at which the search was previously truncated. The

continued search again may not find a root in a finite number of grid points and schedule another virtual collision, or it may now find a collision. In either case the new event is scheduled in the tree. This virtual collision technique avoids the unnecessary computation of a collision time that is so far in the future that it will not be executed in all likelihood anyway, while at the same time ensuring that if, despite the odds, that collision is to happen nonetheless, it is indeed found and correctly executed. The trade-off of this technique is that the event tree is substantially larger, slowing down the event management. Due to the high cost of numerical root searches however, the simulations presented in the accompanying paper showed that using virtual collision events yields an increase in efficiency between 25% and 110%, depending mainly on the system size.

IV. COLLISION RULES

At each moment of collision, the impulsive forces and torques lead to discontinuous jumps in the momenta and angular momenta of the colliding bodies. In the presence of constraints, there are two equivalent ways of deriving the rules governing these changes. In the first approach, the dynamics are treated by applying constraint conditions to Cartesian positions and momenta. This approach is entirely general and is suited for both constrained rigid and non-rigid motion. In its generality, it is unnecessarily complicated for purely rigid systems and is not suitable for continuum bodies. The second approach, suitable for rigid bodies only, uses the fact that only six degrees of freedom, describing the center of mass motion and orientational dynamics are required to fully describe the dynamics of an arbitrary rigid body. The derivation therefore consists of prescribing a collision process in terms of impulsive changes to the velocity of the center of mass and impulsive changes to the angular velocity.

A. Constrained variable approach

The general collision process in systems with discontinuous potentials can be seen as a limit of the collision process for continuous systems in which the interaction potential becomes infinitely steep. A useful starting point for deriving the collision rules is therefore to consider the effect of a force applied to the overall change in the momentum of any atom k:

$$\begin{aligned} \boldsymbol{p}_k' &\equiv \boldsymbol{p}_k(t_c+\Delta t) = \boldsymbol{p}_k + \int_{t_c-\Delta t}^{t_c+\Delta t} \dot{\boldsymbol{p}}_k(t)dt \\ &= \boldsymbol{p}_k + \int_{t_c-\Delta t}^{t_c+\Delta t} \boldsymbol{F}_k(\boldsymbol{r}_N(t))dt, \end{aligned} \tag{67}$$

where $\boldsymbol{F}_k$ is the total force acting on atom k and $\boldsymbol{p}_k \equiv \boldsymbol{p}_k(t_c-\Delta t)$. Furthermore, here and below the pre and post-collision values of a quantity $\boldsymbol{a}$ are denoted by $\boldsymbol{a}$ and $\boldsymbol{a}'$, respectively.

For discontinuous systems, the intermolecular forces are impulsive and occur only at an instantaneous collision time t_c. When atoms i and j collide, the interaction potential Φ depends only on the scalar distance r_{ij} between those atoms, so that the force on an arbitrary atom k is given by (without summation over i and j)

$$\begin{aligned} -\frac{\partial\Phi(\boldsymbol{r}_N)}{\partial \boldsymbol{r}_k} &= -\frac{\partial\Phi(\boldsymbol{r}_N)}{\partial r_{ij}}\frac{\partial r_{ij}}{\partial \boldsymbol{r}_{ij}}\cdot\frac{\partial \boldsymbol{r}_{ij}}{\partial \boldsymbol{r}_k} \\ &= -\frac{\partial\Phi(\boldsymbol{r}_N)}{\partial r_{ij}}\frac{1}{r_{ij}}\boldsymbol{r}_{ij}(\delta_{jk}-\delta_{ik}). \end{aligned}$$

Note that this is non-zero only for the atoms involved in the collision, as expected. Given that the force is impulsive, it may be written as

$$-\frac{\partial\Phi(\boldsymbol{r}_N)}{\partial \boldsymbol{r}_k} = S\,\delta(t-t_c)\hat{\boldsymbol{r}}_{ij}(\delta_{jk}-\delta_{ik}), \tag{68}$$

where the scalar S is the magnitude of the impulse (to be determined) on atom a in the collision.

In general, the constraint forces on the right-hand side of Eq. (7) must also have an impulsive component whenever intermolecular forces are instantaneous in order to maintain the rigid body constraints at all times. We account for this by writing the Lagrange multipliers as

$$\lambda_\alpha = \nu_\alpha + \mu_\alpha\delta(t-t_c).$$

Because λ_α enters into the equations of motion for all atoms k involved in the constraint σ_α, there is an effect of this impulsive constraint force on all those atoms. Thus, one can write for the force on a atom k when atoms i and j collide:

$$\begin{aligned} \boldsymbol{F}_k(\boldsymbol{r}_N) &= -\nu_\alpha\frac{\partial\sigma_\alpha(\boldsymbol{r}_N)}{\partial \boldsymbol{r}_k} \\ &\quad + \delta(t-t_c)\left[S\hat{\boldsymbol{r}}_{ij}(\delta_{jk}-\delta_{ik}) - \mu_\alpha\frac{\partial\sigma_\alpha(\boldsymbol{r}_N)}{\partial \boldsymbol{r}_k}\right]. \end{aligned} \tag{69}$$

Substituting Eq. (69) into (67), one finds that the term proportional to ν_α vanishes in the limit that the time interval Δt approaches zero, so that the post-collision momenta $\boldsymbol{p}_k'$ are related to the pre-collision momenta $\boldsymbol{p}_k$ by

$$\boldsymbol{p}_k' = \boldsymbol{p}_k - \mu_\alpha\frac{\partial\sigma_\alpha(\boldsymbol{r}_N)}{\partial \boldsymbol{r}_k} + S\hat{\boldsymbol{r}}_{ij}(\delta_{jk}-\delta_{ik}). \tag{70}$$

Note that at the instant of collision $t=t_c$, the positions of all atoms $\boldsymbol{r}_N$ remain the same (only their momenta change) so that there is no ambiguity in the right-hand side of Eq. (70) as to whether to take the $\boldsymbol{r}_N$ before or after the collision. It is straightforward to show that due to the symmetry of the interaction potential, the total linear momentum and angular momentum of the system are conserved by the collision rule Eq.(70) for arbitrary

values of the unknown scalar functions S and μ_α. In addition to these constants of the motion, the collision rule must also conserve total energy and preserve the constraint conditions, $\sigma_\alpha(\boldsymbol{r}_N) = 0$ and $\dot{\sigma}_\alpha(\boldsymbol{r}_N) = 0$, before and after the collision. The first constraint condition is trivially satisfied at the collision time, since the positions are not altered at the moment of contact. The second constraint condition allows the scalar μ_α to be related to the value of S using Eq. (9) before and after the collision, since we must have

$$\begin{aligned} \dot{\sigma}_\alpha &= \sum_k \frac{\boldsymbol{p}_k}{m_k} \cdot \frac{\partial \sigma_\alpha}{\partial \boldsymbol{r}_k} = 0 \\ \dot{\sigma}'_\alpha &= \sum_k \frac{\boldsymbol{p}'_k}{m_k} \cdot \frac{\partial \sigma_\alpha}{\partial \boldsymbol{r}_k} = 0. \end{aligned} \tag{71}$$

Inserting Eq. (70) into Eq. (71), one gets

$$0 = \sum_k \frac{1}{m_k} \left(S\hat{\boldsymbol{r}}_{ij}(\delta_{jk} - \delta_{ik}) - \mu_\beta \frac{\partial \sigma_\beta}{\partial \boldsymbol{r}_k} \right) \cdot \frac{\partial \sigma_\alpha}{\partial \boldsymbol{r}_k}. \tag{72}$$

Solving this linear equation for μ_α gives

$$\begin{aligned} &\mu_\alpha = \mathbf{Z}^{-1}_{\alpha\beta} \mathcal{F}_\beta \\ &\mathcal{F}_\beta = S\hat{\boldsymbol{r}}_{ij} \cdot \left(\frac{1}{m_j} \frac{\partial \sigma_\beta}{\partial \boldsymbol{r}_j} - \frac{1}{m_i} \frac{\partial \sigma_\beta}{\partial \boldsymbol{r}_i} \right), \end{aligned} \tag{73}$$

where the $\mathbf{Z}$ matrix was defined in Eq. (12). Note that if atoms i and j are on different bodies, a given constraint σ_β involves either one or the other atom (or neither), so at least one of the two terms on the right-hand side of Eq. (73) is then zero. Equation (70) can now be written as

$$\begin{aligned} \boldsymbol{p}'_k &= \boldsymbol{p}_k + S\Delta\boldsymbol{p}_k \\ \Delta\boldsymbol{p}_k &= \hat{\boldsymbol{r}}_{ij}(\delta_{jk} - \delta_{ik}) - \mu^*_\alpha \frac{\partial \sigma_\alpha}{\partial \boldsymbol{r}_k}, \end{aligned} \tag{74}$$

where $\mu^*_\alpha = \mu_\alpha / S$ is a function of the phase-space coordinate as determined by Eq. (73) and is independent of S.

Finally, the scalar S can be determined by employing energy conservation,

$$\frac{\boldsymbol{p}'_k \cdot \boldsymbol{p}'_k}{2m_k} + \Delta\Phi = \frac{\boldsymbol{p}_k \cdot \boldsymbol{p}_k}{2m_k}, \tag{75}$$

where $\Delta\Phi = \Phi' - \Phi$ denotes the discontinuous change in the potential energy at the collision time. Inserting the expression in (74) into (75) and using Eq. (9), one gets a quadratic equation for the scalar S,

$$\begin{aligned} &aS^2 + bS + \Delta\Phi = 0 \\ &a = \sum_k \frac{\Delta\boldsymbol{p}_k \cdot \Delta\boldsymbol{p}_k}{2m_k} \\ &b = \sum_k \frac{\boldsymbol{p}_k \cdot \Delta\boldsymbol{p}_k}{m_k} = \hat{\boldsymbol{r}}_{ij} \cdot \boldsymbol{v}_{ij}. \end{aligned} \tag{76}$$

For finite values of $\Delta\Phi$, the value of S is therefore

$$S = \frac{-b \pm \sqrt{b^2 - 4a\Delta\Phi}}{2a}, \tag{77}$$

where the physical solution corresponds to the positive (negative) root if $b > 0$ ($b < 0$), provided $b^2 > 4a\Delta\Phi$. If this latter condition is not met, there is not enough kinetic energy to overcome the discontinuous barrier, and the system experiences a hard-core scattering, with $\Delta\Phi = 0$, so that Eq. (77) gives $S = -b/a$. Once the value of S has been computed, the discrete changes in momenta or velocities are easily computed using Eq. (74).

B. Rigid body approach

The solution method outlined above can be applied to semi-flexible as well as rigid molecular systems, but is not very suitable for rigid, continuous bodies composed of an infinite number of point particles. For perfectly rigid molecules, a more convenient approach is therefore to analyze the effect of impulsive collisions on the center of mass and angular coordinates of the system, which are the minimum number of degrees of freedom required to specify the dynamics of rigid systems. The momentum of the center of mass $\boldsymbol{P}_a$ and the angular momentum $\boldsymbol{L}_a$ of rigid molecule a are affected by the impulsive collision via

$$\begin{aligned} \boldsymbol{P}'_a &= \boldsymbol{P}_a + \Delta\boldsymbol{P}_a \\ \boldsymbol{L}'_a &= \boldsymbol{R}_a \times \boldsymbol{P}'_a + \mathbf{I}_a \cdot \boldsymbol{\omega}'_a \\ &= \boldsymbol{L}_a + \boldsymbol{R}_a \times \Delta\boldsymbol{P}_a + \mathbf{I}_a \cdot \Delta\boldsymbol{\omega}_a \\ &= \boldsymbol{L}_a + \Delta\boldsymbol{L}_a, \end{aligned} \tag{78}$$

where $\mathbf{I}_a$ and $\boldsymbol{\omega}_a$ are the moment of inertia tensor and the angular velocity of body a in the laboratory frame, respectively. Note that they are related to their respective quantities in the principal axis frame (body frame) via the matrix $\mathbf{A}_a(t)$ (now associated with the body a):

$$\begin{aligned} \mathbf{I}_a &= \mathbf{A}_a^\dagger \, \tilde{\mathbf{I}}_a \, \mathbf{A}_a \\ \boldsymbol{\omega}_a &= \mathbf{A}_a^\dagger \, \tilde{\boldsymbol{\omega}}_a. \end{aligned} \tag{79}$$

To derive specific forms for the impulsive changes $\Delta\boldsymbol{P}_a$ and $\Delta\boldsymbol{\omega}_a$, one may either calculate the impulsive force and torque acting on the center of mass and angular momentum, leading to $\Delta\boldsymbol{P}_a = -\Delta\boldsymbol{P}_b = -S\hat{\boldsymbol{r}}$ and $\Delta\boldsymbol{L}_a = -\Delta\boldsymbol{L}_b = \boldsymbol{r}_a \times \Delta\boldsymbol{P}_a$, where $\boldsymbol{r}_a$ and $\boldsymbol{r}_b$ are the points at which the forces are applied on body a and b, respectively, while $\hat{\boldsymbol{r}} = (\boldsymbol{r}_b - \boldsymbol{r}_a)/|\boldsymbol{r}_b - \boldsymbol{r}_a|$, and S should be obtained from energy conservation. To understand this better and make a connection with the previous section, one may equivalently view the continuum rigid body as a limit of a non-continuum rigid body composed of n constrained point particles, and use the expressions derived in the previous section for the changes in momenta of the constituents.

In the latter approach, it is convenient to switch the notation for the positions and momenta of the atoms from $\boldsymbol{r}_i$ and $\boldsymbol{p}_i$ to $\boldsymbol{r}_i^a$ and $\boldsymbol{p}_i^a$, which indicate the position and momentum of particle i on body a, respectively. Using this notation and considering a collision between particle i on body a and particle j on body b, Eq. (74) can be written as

$$\boldsymbol{p}_k^{a\prime} - \boldsymbol{p}_k^a = S\Delta\boldsymbol{p}_k^a = -S\left[\hat{\boldsymbol{r}}_{ij}^{ab}\delta_{ik} + \mu_\alpha^* \frac{\partial\sigma_\alpha}{\partial \boldsymbol{r}_k}\right], \qquad (80)$$

where $\hat{\boldsymbol{r}}_{ij}^{ab} = \boldsymbol{r}_{ij}^{ab}/r_{ij}^{ab}$ is the unit vector along the direction of the vector $\boldsymbol{r}_{ij}^{ab} = \boldsymbol{r}_j^b - \boldsymbol{r}_i^a$ connecting atom i on body a with its colliding partner j on body b. Thus, noting that $\boldsymbol{R}_a = \sum_k m_k^a \boldsymbol{r}_k^a/M_a$, where $M_a = \sum_{k=1}^n m_k^a$ is the total mass of body a, and using Eq. (80), one finds that

$$\begin{aligned} \boldsymbol{P}_a' &= \boldsymbol{P}_a + \Delta\boldsymbol{P}_a \qquad (81)\\ \Delta\boldsymbol{P}_a &= S\sum_{k=1}^n \Delta\boldsymbol{p}_k^a = -S\mu_\alpha^* \sum_{k=1}^n \frac{\partial\sigma_\alpha}{\partial\boldsymbol{r}_k} - S\hat{\boldsymbol{r}}_{ij}^{ab} = -S\hat{\boldsymbol{r}}_{ij}^{ab}, \end{aligned}$$

since

$$\sum_{k=1}^n \frac{\partial\sigma_\alpha(\boldsymbol{r}_{uv})}{\partial\boldsymbol{r}_k} = \sum_{k=1}^n \sigma_\alpha'\hat{\boldsymbol{r}}_{uv}\left(\delta_{ku} - \delta_{kv}\right) = 0. \qquad (82)$$

Similarly, one finds that

$$\begin{aligned} \Delta\boldsymbol{L}_a &= S\sum_{k=1}^n \boldsymbol{r}_k^a \times \Delta\boldsymbol{p}_k^a \\ &= S\sum_{k=1}^n \left(\boldsymbol{R}_a + \overline{\boldsymbol{r}}_k^a\right) \times \Delta\boldsymbol{p}_k^a \\ &= \boldsymbol{R}_a \times \Delta\boldsymbol{P}_a + S\sum_{k=1}^n \overline{\boldsymbol{r}}_k^a \times \Delta\boldsymbol{p}_k \\ &= \boldsymbol{R}_a \times \Delta\boldsymbol{P}_a - S\,\overline{\boldsymbol{r}}_i^a \times \hat{\boldsymbol{r}}_{ij}^{ab}, \qquad (83) \end{aligned}$$

where $\overline{\boldsymbol{r}}_k^a = \boldsymbol{r}_k^a - \boldsymbol{R}_a$. Comparing with Eq. (78), it is evident that

$$\Delta\boldsymbol{\omega}_a = -S\,\mathbf{I}_a^{-1}\left(\overline{\boldsymbol{r}}_i^a \times \hat{\boldsymbol{r}}_{ij}^{ab}\right). \qquad (84)$$

Note that $\mathbf{I}_a^{-1}$ is a matrix inverse. Once again the impulsive changes are directly proportional to S, and the change of the angular velocity of body b in the laboratory frame due to the collision can be calculated analogously.

To determine the scalar S, one again uses the conservation of total energy ($E' = E$) to see that

$$\begin{aligned} &\frac{|\boldsymbol{P}_a'|^2}{2M_a} + \frac{|\boldsymbol{P}_b'|^2}{2M_b} + \frac{1}{2}\boldsymbol{\omega}_a' \cdot \mathbf{I}_a\,\boldsymbol{\omega}_a' + \frac{1}{2}\boldsymbol{\omega}_b' \cdot \mathbf{I}_b\,\boldsymbol{\omega}_b' + \Delta\Phi \\ &= \frac{|\boldsymbol{P}_a|^2}{2M_a} + \frac{|\boldsymbol{P}_b|^2}{2M_b} + \frac{1}{2}\boldsymbol{\omega}_a \cdot \mathbf{I}_a\,\boldsymbol{\omega}_a + \frac{1}{2}\boldsymbol{\omega}_b \cdot \mathbf{I}_b\,\boldsymbol{\omega}_b. \qquad (85) \end{aligned}$$

Inserting Eqs. (81) and (84) into the energy equation above yields, after some manipulation, a quadratic equation for S of the form of Eq. (77), with

$$\begin{aligned} a &= \frac{1}{2M_a} + \frac{1}{2M_b} + \frac{\Delta E_\omega^a + \Delta E_\omega^b}{2} \\ b &= \boldsymbol{v}_{ij}^{ab} \cdot \hat{\boldsymbol{r}}_{ij}^{ab}, \end{aligned}$$

where

$$\begin{aligned} \Delta E_\omega^a &= \boldsymbol{n}_{ij}^a \cdot \mathbf{I}_a^{-1}\,\boldsymbol{n}_{ij}^a \\ \Delta E_\omega^b &= \boldsymbol{n}_{ij}^b \cdot \mathbf{I}_b^{-1}\,\boldsymbol{n}_{ij}^b, \end{aligned}$$

with

$$\begin{aligned} \boldsymbol{n}_{ij}^a &= \overline{\boldsymbol{r}}_i^a \times \hat{\boldsymbol{r}}_{ij}^{ab} \\ \boldsymbol{n}_{ij}^b &= \overline{\boldsymbol{r}}_j^b \times \hat{\boldsymbol{r}}_{ij}^{ab}. \end{aligned}$$

For a spherically symmetric system, $\mathbf{I} = \tilde{\mathbf{I}} = I_1\mathbb{1}$, and $\Delta E_\omega^{a,b} = \boldsymbol{n}_{ij}^{a,b\dagger} \cdot \boldsymbol{n}_{ij}^{a,b}/I_1$.

V. DYNAMICS IN THE CANONICAL AND MICROCANONICAL ENSEMBLES

Any event-driven molecular dynamics simulation relies on the assumption that no collision is ever missed. However, collisions will be missed whenever the time difference between two nearby events is on the order of (or smaller than) the time error of the scheduled events, which indicates that there is still a finite chance that a collision is missed even when event times are calculated in a simulation starting from an analytic expression, due to limits on machine precision. Although this subtle issue is not very important in a hard sphere system, in the present context it is of interest. Indeed, the extensive use of numerical root searches for the event time calculations combined with the need for computational efficiency demands a lower precision in the time values of collision events (typically a precision of 10^{-10} instead of 10^{-16} for analytical roots). In this section, it will be shown how to handle missed collisions in the context of the hybrid Monte Carlo scheme (HMC).

In general, the HMC method [46, 47] combines the Monte Carlo method with molecular dynamics to construct a sequence of independent configurations $\{\boldsymbol{r}_N^{(1)}, \ldots, \boldsymbol{r}_N^{(n)}\}$, distributed according to the canonical probability density

$$\rho(\boldsymbol{r}_N) = \frac{1}{Z}\exp\left[-\frac{\Phi(\boldsymbol{r}_N)}{k_\mathrm{B}T}\right], \qquad (86)$$

where Z is the configurational integral, k_B is Boltzmann's constant, and T is the temperature. In the present context, this method can be implemented as follows: Initially, a new set of momenta $\boldsymbol{p}_N'$ is selected by choosing a random center of mass momentum $\boldsymbol{P}$ and angular velocity $\boldsymbol{\omega}$ for each molecule from the Gaussian distribution

$$\rho_G \propto \exp\left[-\frac{1}{k_\mathrm{B}T}\left(\frac{|\boldsymbol{P}|^2}{2M} + \frac{1}{2}\boldsymbol{\omega}\cdot\mathbf{I}\,\boldsymbol{\omega}\right)\right].$$

The system is then evolved deterministically through phase-space for a fixed time τ_0 according to the equations of motion. This evolution defines a mapping of phase-space given by $(\boldsymbol{r}_N(0), \boldsymbol{p}_N(0)) \mapsto$

$(\boldsymbol{r}_N(\tau_0), \boldsymbol{p}_N(\tau_0)) \equiv (\boldsymbol{r}'_N, \boldsymbol{p}'_N)$. The resulting phase space point $(\boldsymbol{r}'_N, \boldsymbol{p}'_N)$ and trajectory segment are then accepted with probability

$$p_A(\boldsymbol{r}'_N, \boldsymbol{p}'_N | \boldsymbol{r}_N(0), \boldsymbol{p}_N(0)) = \min\left\{1, \exp\left[-\frac{\Delta E}{k_{\rm B}T}\right]\right\}, \tag{87}$$

where

$$\Delta E = E(\boldsymbol{r}'_N, \boldsymbol{p}'_N) - E(\boldsymbol{r}_N(0), \boldsymbol{p}_N(0)), \tag{88}$$

and

$$E(\boldsymbol{r}_N, \boldsymbol{p}_N) = \sum_{i=1}^{N} \frac{1}{2m_i}|\boldsymbol{p}_i|^2 + \Phi(\boldsymbol{r}_N). \tag{89}$$

This algorithm generates a Markov chain of configurations with an asymptotic distribution given by the stationary canonical distribution defined in Eq. (86) provided that the phase space trajectory is *time reversible* and *area preserving*[46]. Since free translational motion is time reversible, and the reversibility of the rotational equations of motion is evident from Eq. (30), the first requirement is satisfied. Furthermore, since the invariant phase space metric is uniform for fully rigid bodies (see Eq. (14) in Sec. II A), the *area preserving* condition is also satisfied.

Ideally, a DMD simulation satisfies $\Delta E = 0$ so that according to Eq. (87) every trajectory segment is accepted. In the less ideal, more realistic case in which collisions are occasionally missed, the HMC scheme provides a rigorous way of accepting or rejecting the segment. If a hard-core collision has been missed and the configuration at the end of a trajectory segment has molecules in unphysical regions of phase space where the potential energy is infinite, then $\Delta E = \infty$ and the new configuration and trajectory segment are always rejected. On the other hand, if only a square-well interaction has been missed, ΔE at the end of the trajectory segment is finite and there is a non-zero probability of accepting the trajectory.

An analogous strategy can be devised to carry out microcanonical averages. In this case, the assignment of new initial velocities in the first step is still done randomly but in such a way that the total kinetic energy of the system remains constant. Such a procedure can be carried out by exchanging center of mass velocities between randomly chosen pairs of molecules. The system is evolved dynamically through phase space for a fixed time τ_0 and the new phase space point $(\boldsymbol{r}'_N, \boldsymbol{p}'_N)$ is accepted according to

$$p_A\left(\boldsymbol{r}'_N, \boldsymbol{p}'_N | \boldsymbol{r}_N(0), \boldsymbol{p}_N(0)\right) = \begin{cases} 0 & \text{if } \Delta E \neq 0 \\ 1 & \text{if } \Delta E = 0, \end{cases} \tag{90}$$

where ΔE is given by Eq. (88). Clearly, the case $\Delta E \neq 0$ only occurs when a collision has been missed, and in such a case the trajectory segment is never accepted.

It should be emphasized that in the HMC scheme, a new starting configuration for a segment of time evolution is chosen only after every DMD time interval τ_0. An algorithm in which a new configuration is selected only after a collision is missed is likely to violate detailed balance, and is therefore not a valid Monte-Carlo scheme. On the other hand, the length of the trajectory segments τ_0 in the HMC method outlined above can be chosen to be slightly larger than the relevant relaxation time of the system. Such a choice allows one to use the deterministic phase space trajectory to compute time-dependent correlation functions from the *exact* dynamics of the system without rejecting a significant fraction of the trajectory segments.

VI. CONCLUSIONS

In this paper we have shown how to carry out discontinuous molecular dynamics simulations for arbitrary semi-flexible and rigid molecules. For semi-flexible bodies, the dynamics and collision rules have been derived from the principles of constrained Lagrangian mechanics. The implementation of an efficient DMD method for semi-flexible systems is hindered by the fact that in almost all cases the equations of motion must be propagated numerically in an event searching algorithm so that the constraints are enforced at all times. Nonetheless, such a scheme can be realized using the SHAKE[28] or RATTLE[48] algorithms in combination with the root searching methods outlined here.

The dynamics of a system of completely rigid molecules interacting through discontinuous potentials is more straightforward. For such a system, the Euler equations for rigid body dynamics can be used to calculate the free evolution of a general rigid object. This analytical solution enables the design of efficient numerical algorithms for the search for collision events. In addition, the collision rules for calculating the discontinuous changes in the components of the center of mass velocity and angular momenta have been obtained for arbitrary bodies interacting through a point based on conservation principles. Furthermore, the sampling of the canonical and microcanonical ensembles, as well as the handling of missed collisions, has also been discussed in the context of a hybrid Monte Carlo scheme.

From an operational standpoint, the difference between the method of DMD and molecular dynamics using continuous potentials in rigid systems lies in the fact that the DMD approach does not require the calculation of forces and sequential updating of phase space coordinates at discrete (and short) time intervals since the response of the system to an impulse can be computed analytically. Instead, the computational effort focuses on finding the precise time at which such impulses exert their influence. The basic building block outlined here for the numerical computation of collision times is a grid search, for which the positions of colliding atoms on a given pair of molecules need to be computed at equally spaced points in time. As outlined in Sec. III, this can be done efficiently starting with a completely explicit an-

alytical form of the motion of a torque-free rigid body, without which the equations of motions would have to be integrated numerically. An efficient implementation of the DMD technique to find the time collision events should make use of a) a large grid step combined with a threshold scenario to catch pathological cases, b) sophisticated but standard techniques such as binary event trees, cell divisions, and local clocks, and c) a new technique of finding collision times numerically that involves truncating the grid search and scheduling virtual collision events.

On a fundamental level, it is natural to wonder whether the 'stepped' form of a discontinuous potential could possibly model any realistic interaction. Such concerns are essentially academic, since it is always possible to approximate a given interaction potential with as many (small) steps as one would like in order to approximate a given potential to any desired level of accuracy[6]. Of course, the drawback to mimicking a smooth potential with a discontinuous one with many steps is that the number of 'collision' events that occur in the system per unit time scales with the number of steps in the potential. Hence, one would expect that the efficiency of the simulation scales roughly inversely with the number of steps in the interaction potential. Nonetheless, the issue is a practical one: How small can the number of steps in the interaction potential be such that one still gets a good description of the physics under investigation? In the accompanying paper[49], we will see for benzene and methane that it takes surprisingly few steps (e.g. a hard core plus a square-well interaction) to get results which are very close to those of continuous molecular dynamics. Additionally, we compare the efficiency of such simulations to simulations based on standard molecular dynamics methods.

VII. ACKNOWLEDGMENTS

The authors would like to acknowledge support by grants from the Natural Sciences and Engineering Research Council of Canada (NSERC).

[1] B. J. Alder and T. E. Wainwright, J. Chem. Phys. **31**, 459 (1959).

[2] B. J. Alder and T. E. Wainwright, J. Chem. Phys. **33**, 1439 (1960).

[3] M. P. Allen and D. J. Tildesley, *Computer simulation of liquids* (Clarendon Press, New York, NY, USA, 1987).

[4] M. P. Allen, D. Frenkel, and J. Talbot, Comput. Phys. Rep. **9**, 301 (1989).

[5] D. C. Rapaport, *The Art of Molecular Dynamics Simulation* (Cambridge University Press, Cambridge, 2004).

[6] G. A. Chapela, H. T. Davis, and L. E. Sciven, Chemical Physics **129**, 201 (1989).

[7] G. A. Chapela, S. E. Martínez-Casas, and J. Alejandre, Molecular Physics **53**, 139 (1984).

[8] R. van Zon and J. Schofield, Phys. Rev. E **65**, 011107 (2002).

[9] A. S. Rueb, Ph.D. thesis, Trajecti ad Rhenum (i.e. Utrecht, Netherlands) (1834).

[10] C. G. J. Jacobi, Crelle J. Reine Angew. Math. **39**, 293 (1849).

[11] E. T. Whittaker, *A Treatise on the Analytical Dynamics of Particles and Rigid Bodies* (Cambridge University Press, 1937), 4th ed.

[12] L. D. Landau and E. M. Lifshitz, *Mechanics* (Pergamon Press, 1976), 3rd ed.

[13] J. E. Marsden and T. S. Ratiu, *Introduction to Mechanics and Symmetry: A Basic Exposition of Classical Mechanical Systems* (Springer, New York, 2002), 2nd ed.

[14] Y. Masutani, T. Iwatsu, and F. Miyazaki, in *Proc. IEEE Int. Conf. on Robotics and Automation* (IEEE Computer Society Press, 1994), pp. 1066–1072, vol. 2.

[15] G. Ciccotti and G. Kalibaeva, J. Stat. Phys. **115**, 701 (2004).

[16] A. Donev, S. Torquato, and F. H. Stillinger, J. Comput. Phys. **202**, 737 (2005).

[17] A. Donev, S. Torquato, and F. H. Stillinger, J. Comput. Phys. **202**, 765 (2005).

[18] C. De Michele, S. Gabrielli, P. Tartaglia, and F. Sciortino, J. Phys. Chem. B **110**, 8064 (2006).

[19] L. Hernández de la Peña, R. van Zon, J. Schofield, and S. B. Opps, *Discontinuous molecular dynamics simulations of water*, in preparation.

[20] H. Goldstein, *Classical Mechanics* (Addison-Wesley, Reading, Massachusetts, 1980).

[21] To be more precise, no Hamiltonian exists with $\boldsymbol{r}_i$ and $\boldsymbol{p}_i$ as conjugate variables. Otherwise, $\dot{\boldsymbol{r}}_i$ should be equal to $\partial\mathcal{H}/\partial\boldsymbol{p}_i$ and $\dot{\boldsymbol{p}}_i$ should be equal to $-\partial\mathcal{H}/\partial\boldsymbol{r}_i$, whence $\partial\dot{\boldsymbol{r}}_i/\partial\boldsymbol{r}_i = -\partial\dot{\boldsymbol{p}}_i/\partial\boldsymbol{p}_i$, but Eq. (13) violates this relation.

[22] J. D. Ramshaw, Phys. Lett. A **116**, 110 (1986).

[23] M. E. Tuckerman, C. J. Mundy, and G. J. Martyna, Europhys. Lett. **45**, 149 (1999).

[24] M. E. Tuckerman, Y. Liu, G. Ciccotti, and G. J. Martyna, J. Chem. Phys. **115**, 1678 (2001).

[25] S. Melchionna, Phys. Rev. E **61**, 6165 (2000).

[26] M. Fixman, Proc. Natl. Acad. Sci. U.S.A. **71**, 3050 (1974).

[27] E. A. Carter, G. Ciccotti, J. T. Hynes, and R. Kapral, Chem. Phys. Lett. **156**, 472 (1989).

[28] J.-P. Ryckaert, G. Ciccotti, and H. J. C. Berendsen, J. Comp. Phys. **23**, 327 (1977).

[29] R. van Zon and J. Schofield, *Numerical implementation of the exact dynamics of free rigid bodies*, cond-mat/0607529.

[30] E. T. Whittaker and G. N. Watson, *A Course of Modern Analysis* (Cambridge University Press, 1927), 4th ed.

[31] M. Abramowitz and I. A. Stegun, *Handbook of Mathematical Functions with formulas, graphs, and mathematical tables* (Dover, New York, 1965).

[32] W. H. Press, S. A. Teukolsky, W. T. Vetterling, and B. P. Flannery, *Numerical Recipes in Fortran, The Art of Scientific Computing* (Cambridge University Press, Cambridge, 1992), 2nd ed.

[33] S. L. Moshier, *Methods and Programs for Mathematical*

Functions (Ellis Horwood Limited, New York, 1989).
[34] M. Galassi, J. Davies, J. Theiler, B. Gough, G. Jungman, M. Booth, and F. Rossi, *GNU Scientific Library Reference Manual* (Network Theory Ltd, Bristol, 2005), revised 2nd ed.
[35] K. Knopp, *Theory of Functions: Part II* (Dover, Mineola, NY, 1947).
[36] D. Baraff, Ph.D. thesis, Cornell University (1992).
[37] D. Baraff, Computer Graphics **23**, 223 (1989).
[38] The threshold value is found by trial and error; a trial simulation with a very small threshold value is run which is sure to miss a collision at some point due to a grazing collision; the collision indicator function around the time of this grazing collision is inspected and the threshold value is adjusted such that this collision will not be missed. New trial simulation are run, and the threshold adjusted, until the frequency of missed grazing collisions is acceptable.
[39] R. P. Brent, *Algorithms for Minimization without Derivatives* (Prentice Hall, Englewood Cliffs, New Jersey, 1973).
[40] This assumes no optimization whatsoever. It is easy to reduce the cost of finding the first possible collision times to $O(N^2)$ per unit physical time, however, by storing only the first collision for every given particle[3].
[41] J. J. Erpenbeck and W. W. Wood, in *Statistical Mechanics Part B*, edited by B. J. Berne (Plenum, New York, 1977).
[42] D. C. Rapaport, J. Comp. Phys. **34**, 184 (1980).
[43] B. D. Lubachevsky, J. Comput. Phys. **94**, 255 (1991).
[44] M. Marin, D. Risso, and P. Cordero, J. Comput. Phys. **109**, 306 (1993).
[45] M. Marin and Cordero, Comp. Phys. Comm. **92**, 214 (1995).
[46] S. Duane, A. D. Kennedy, B. J. Pendleton, and D. Roweth, Phys. Lett. B **195**, 216 (1987).
[47] D. B. Mehlig, D. W. Hermann, and B. M. Forrest, Phys. Rev. B **45**, 679 (1992).
[48] H. C. Andersen, J. Comput. Phys. **52**, 24 (1983).
[49] L. Hernández de la Peña, R. van Zon, J. Schofield, and S. B. Opps, *Discontinuous molecular dynamics for rigid bodies: Applications*, following paper (cond-mat/0607528).